Dr. Stefan Mangold
Lovefield Wireless GmbH, Switzerland
www.lovefield.ch
stefan.mangold@lfield.ch

Assessing the Interference of Miniature Radar on Millimeter Wave 60 GHz Wi-Fi — Supplemental Analysis

June-08, 2018

Summary

1. This document supplements a study that accompanied Google LLC's Request for Waiver of Power Levels for Project Soli filed at the Federal Communications Commission on March 7, 2018.
2. There are four main additions to the original simulation study. First, the Wi-Fi system model now specifically models the single-carrier modulation and coding schemes of 60 GHz Wi-Fi. Second, the study now accounts for the fact that the radar is out of band of the WiFi channel for 75% of the time that the radar is actively transmitting. Third, for increased refinement, a non-line-of-sight path loss channel model taken from IEEE 802.11ad standardization is used in addition to the original free space line-of-sight channel model. Fourth, an additional scenario is added in which the radar devices and Wi-Fi stations are positioned so that outlier circumstances such as close proximities between interferer and victim can be better identified.
3. After making these additions, the main findings are consistent with those of the first study:
   (i) For the typical indoor scenario and with both path loss channel models, the Wi-Fi throughput is only marginally affected by interference from the radar (around 10% throughput reduction and generally far less, if any at all).
   (ii) Radar duty cycling further helps the radar to efficiently coexist with 60 GHz Wi-Fi.
   (iii) In outlier short range scenarios with co-located devices in close proximity to each other, a radar interferer can create additional interference, but only during in-band operation, as duty cycling of the radar mitigates this effect.
   (iv) Simulated throughput results match laboratory measurements with commercially available IEEE 802.11ad equipment.

Table of Contents

Introduction 3

Purpose and Limitation of this Analysis 3

Document Outline 4

Path Loss Channel Model 5

60 GHz Wi-Fi Single Carrier Model 7

60 GHz Wi-Fi with Single Carrier (SC) Modulation and Coding Scheme (MCS) 7

SC Simulation Model 9

Bit Error Ratio (BER) 9

Sensitivity 10

Code Word (Packet) Error Probability and Channel Capacity 11

Evaluation 11

Interference Model 15

Simulation Results 18

Scenario TYPICAL 19

Scenario SHORT_RANGE 22

Model Validation 25

Summary and Final Remarks 27

References 28

Appendix A: Erratum to Mangold (2018) 29

Appendix B: Implementation Details 30

1. Introduction

An earlier study (Mangold, 2018) analyzed the interference effects of a radar system on 60 GHz Wi-Fi. This supplementary analysis presents additional simulation results to provide further insights. Different kinds of 60 GHz Wi-Fi systems, with different channel models, and other scenario configurations are investigated by this supplemental analysis.

An extended Wi-Fi system model is introduced that contains the IEEE 802.11ad single carrier (SC) modulation and coding schemes (MCSs) (IEEE 802.11ad, 2014 and IEEE 802.11, 2016), in addition to the MCSs using Orthogonal Frequency-Division Multiplexing (OFDM) considered in the earlier study. Thus, Wi-Fi devices with SC MCS that were offered in the market earlier and are more likely to be commercially available are addressed.

The supplemental analysis also highlights short range scenarios with devices in close proximity to each other. These additional scenarios offer a better understanding of extreme cases (very short range, no duty cycle), independently of how likely or unlikely such scenarios are to actually occur.

The extended radar system model used for this supplemental study is refined by including a simple in-band time assumption, because approximately 75 % of the time the Continuous Wave (CW) radar will operate out-of-band of the Wi-Fi channel.

Finally, this supplemental study contains both a free space line-of-sight path loss channel model (as in the earlier study) and a non-line-of-sight model. Both path loss models are derived from simulation models taken from IEEE 802.11ad standardization documents (Maltsev et.al., 2008 and Maltsev et.al., 2010).

1.1. Purpose and Limitation of this Analysis

This study is intended to offer interference analysis detailed enough to advance discussions concerning spectral coexistence between radars and Wi-Fi at 60 GHz, while remaining simple enough to allow readers to understand and evaluate the full model. The models underlying the Monte Carlo simulations are based on standard link budget models that are typically used when designing wireless networks, to assess link qualities, or to evaluate spectral coexistence of radio networks. Some radio parameters, such as the effect of multipath propagation, are only approximated in the path loss channel models. Other system behavior parameters, such as protocols or algorithms for dynamic radio resource management (for example, IEEE 802.11 distributed coordination function, power control, link adaptation, dynamic channel selection), are omitted to retain the model's simplicity and because they lack relevance to the analysis. While an alternative modelling approach based on, for example,

ray-tracing or real life measurements, theoretically would be possible, it also could become cost-prohibitive and inefficient given the large number of interference configurations potentially covered by the simulation. To achieve statistical relevance, typically between 20'000 and 50'000 samples are required for one parameter distribution. Relevant implementation details can be found in the Appendix.

1.2. Document Outline

The channel model used in this study is described in Section 2.

Section 3 describes the study's detailed model of the IEEE 802.11ad SC MCS. This section contains a basic evaluation of the theoretical performance of IEEE 802.11ad SC MCS, given the system model and channel model assumptions taken herein. This performance analysis does not analyze interference from radars.

Section 4 contains the description of how the narrow-band continuous wave radar interference and its effect on Wi-Fi are modelled. The simulation results that analyze the interference are presented and discussed in Section 5.

Section 6 contains a brief model validation and a comparison of the simulation results to laboratory measurements.

Section 7 concludes with final remarks, followed by a list of references.

The Appendix contains an erratum to the study that accompanied Google LLC's Request for Waiver of Power Levels for Project Soli filed at the Federal Communications Commission on March 7, 2018. The Appendix also provides implementation details of the simulation model used herein.

2. Path Loss Channel Model

In coexistence studies, simulation results depend on the accurate assessment of signal and interference power levels measured at the antenna of a victim radio station. Distance-dependent signal attenuations are modelled with a simple path loss approximation. An empirically derived path loss model, intended to assist simulation studies of IEEE 802.11ad, can be found in Maltsev et.al. (2009). A number of scenarios are defined in Maltsev et.al. (2009), for which the path loss model parameters are modified to match real life propagation characteristics. Two of the scenarios are used in this study: "*Living Room, LOS*" and "*Living Room, NLOS.*" Maltsev et.al, (2009).

Equation 1 describes the model of the simulation study. The reference distance chosen is 0.5 meters, below which no change of signal attenuation when compared to the reference distance is taken into account. This is a common solution to approximate short distance attenuations close to the antenna near fields (Rappaport, 2008).

Table 3 summarizes parameter values. Figure 1 illustrates the resulting signal to noise ratios in the absence of radar interference, which is analyzed later in this document. For simplicity's sake, shadow fading variations, as proposed for NLOS in the original sources, are not taken into account (zero standard deviation) during simulation.

Link budget models include gains of the transmitter and receiver antennas. The antenna gain depends on the antenna's direction. In this study (if not otherwise defined), it is assumed that the radar antenna points to an arbitrary, randomly chosen direction in azimuth that changes with each experiment. The Wi-Fi transmitter antenna at the access point and the receiver antenna at the station are assumed to be identical and directed towards each other. There is no third dimension, i.e., no modelling of signal emissions in elevation. See Figure 2 for an illustration of the antenna patterns.

$$PL[dB] = A + 20 \cdot \log_{10}\left(\frac{f_c}{1\,Hz}\right) + \begin{cases} 10 \cdot n \cdot \log_{10}\left(\frac{r}{1\,m}\right) & \text{for } r \geq 0.5\,m \\ 10 \cdot n \cdot \log_{10}\left(\frac{1}{2}\right) & \text{for } r < 0.5\,m \end{cases} \qquad \textbf{(Equation 1)}$$

Model	f_c [GHz]	A [dB]	n	Std. Dev. Shadow Fading
LOS	60.48	32.5	2.0	0
NLOS	60.48	44.7	1.5	0

Table 1: Path loss model parameters.

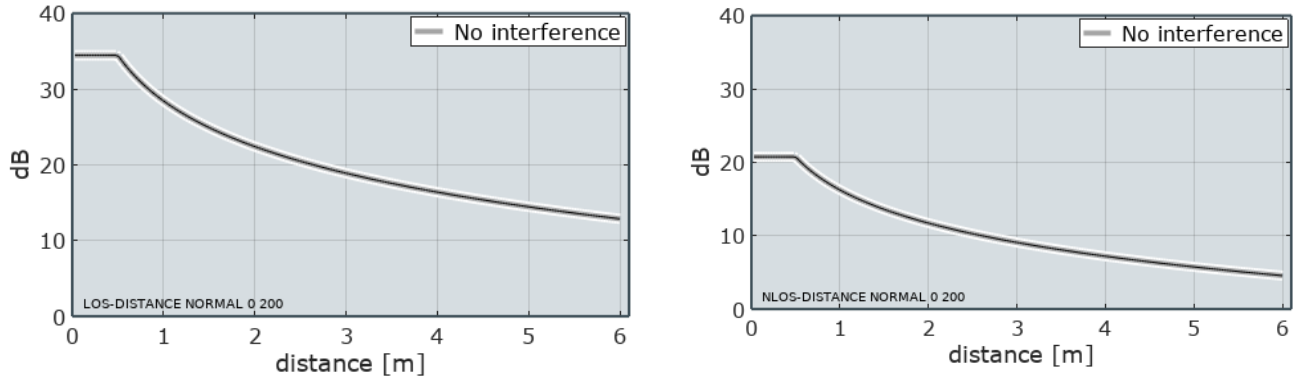

(a) LOS (b) NLOS

Figure 1: Signal to noise (Eav/N0) ratio over distance between radio devices (Wi-Fi or radar) for two channel models. The effect of the reference distance (0.5 m) and the influence of parameter A in both models can be observed.

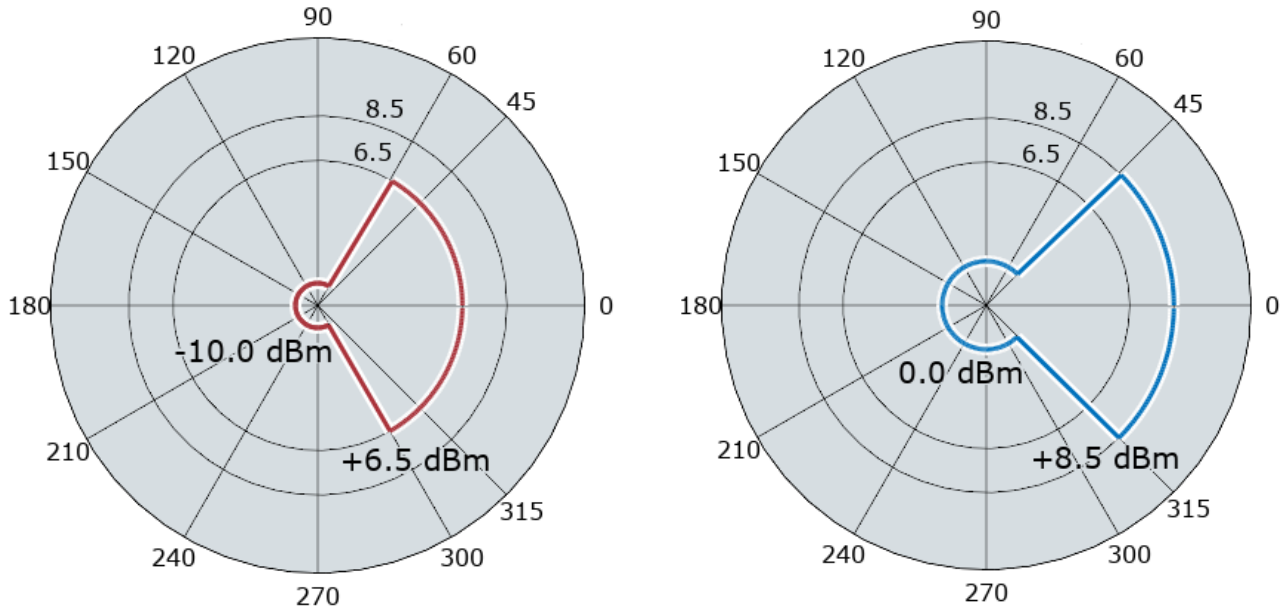

(a) Radar transmitter antenna

(b) Wi-Fi transmitter and receiver antenna (90 degree angle, four antenna sectors).

Figure 2: Radar and Wi-Fi 2-D antenna patterns as used in the simulation. Wi-Fi 60GHz antennas operate with antenna sectors. The 90 degree beam angle indicated in Figure (b) leads to four antenna sectors. The number of sectors available to a station depends on the directionality of the station's antenna, and is increased by increasing the number of antenna elements that are deployed in a station. Nitsche et.al. (2014) claim that 1 ... 32 elements are common in consumer devices such as smartphones, handheld devices, tablets or notebooks. Therefore, four antenna sectors (90 degree angle) are chosen here as a conservative approach to model most types of consumer devices. Note that the back-lobe gain of the Wi-Fi antenna is conservatively chosen to be quite large (0 dB), which makes the Wi-Fi device more vulnerable to interference in the study than is expected in practice.

3. 60 GHz Wi-Fi Single Carrier Model

This section describes the mathematical model of the 60 GHz Wi-Fi system used in this study. Section 3.1 summarizes the system parameters. Section 3.2 describes the model and contains figures showing the theoretical performance in the presence of thermal noise (without any radar interference).

3.1. 60 GHz Wi-Fi with Single Carrier (SC) Modulation and Coding Scheme (MCS)

Whereas Mangold (2018) studies the 60 GHz Wi-Fi with OFDM multicarrier modulation, this study examines the impact of the radar on the SC Modulation and Coding Schemes (MCS 1 to MCS 12) of IEEE 802.11ad (IEEE 802.11ad, 2014 and IEEE 802.11, 2016).

Channel bandwidth and center frequency	2160 MHz | 60.48 GHz
Signal bandwidth (-17 dBr transmit mask)	1880 MHz
Symbol rate ("SC chip rate" in 802.11ad)	1760 MHz
Symbol duration ("SC chip time" in 802.11ad)	1/1760 MHz = 0.56818 ns
Modulation	**π/2-BPSK** | **π/2-QPSK** | **π/2-16QAM**
Physical layer bitrate (modulated, no coding)	1760.0 Mbps | 3520.0 Mbps | 7040.0 Mbps
LDPC code rate MCS 1	1/4 **(repetition, with code rate 1/2)**
LDPC code rate MCS 2 … 12	1/2, 5/8, 3/4, 13/16
LDPC code word size	672 bit
LDPC coding gain (approx.)	**Rate 1/4:** 8.0 dB | **1/2:** 6.0 dB | **5/8:** 4.0 dB **Rate 3/4:** 3.0 dB | **13/16:** 3.2 dB
Physical layer bitrate (LDPC encoded data)	440.0 Mbps **(MCS1)** … 5280.0 Mbps **(MCS12)**
Block size (BPSK | QPSK | 16-QAM)	448 bit | 896 bit | 1792 bit
Block duration (encoded data only)	254.55 ns
Golay sequence preceding each block	64 BPSK symbols (64 bit) | **duration:** 36.364 ns
Block duration (LDPC encoded data + Golay)	290.91 ns
Physical layer bitrate (LDPC encoded data + Golay)	385.0 Mbps **(MCS1)** … 4620.0 Mbps **(MCS12)**
Tx and Rx antenna beamform gain	8.5 dBi
Transmission peak power	**Used in this study:** 150 mW (21.76 dBm) EIRP **FCC limit:** 20 W (43.00 dBm) EIRP
Receiver implementation loss and noise figure N_f	15 dB

Table 2: 60 GHz Wi-Fi with SC modulation and coding schemes (mandatory MCS 1 … MCS 4, and the optional MCS 5 … MCS 12 in IEEE 802.11ad, 2014).

MCS	1	2	3	4	5	6	7	8	9	10	11	12
Sensitivity (1 % PER) [dBm]	-78	-68	-66	-65	-64	-62	-63	-62	-61	-59	-55	-54
Cut-off sensitivity $P_{rx,cutoff}$ (100 % PER) [dBm]	-81	-71	-69	-68	-67	-65	-66	-65	-64	-62	-58	-57

Table 3: 60 GHz Wi-Fi receiver sensitivities for MCS 1 to MCS 12. The sensitivities are defined in IEEE 802.11ad (2014) for levels that lead to a Packet Error Rate (PER) of 1 %. For the model, a cut-off sensitivity level is introduced and used.

Technical details of the SC MCS relevant to this study are given in Table 2 and Table 3. Figure 3 illustrates the operation in four frequency channels. Wi-Fi packets are assumed to be constructed with a number of consecutive SC symbols. This assumption leaves out special intervals such as ranging and synchronization phases, or transmissions with MCSs that are not SC.

In real life scenarios, Wi-Fi packet lengths depend on higher layer protocols and the payload size of the original data, and could vary significantly. The encoding also could change throughout the transmission of a Wi-Fi packet, from one symbol to the next, as some symbols that are required for reliable operation are transmitted at more robust and mandatory MCSs. All evaluations in this study assume operation on channel 2, which ITU-R recommends to be used as the default channel.

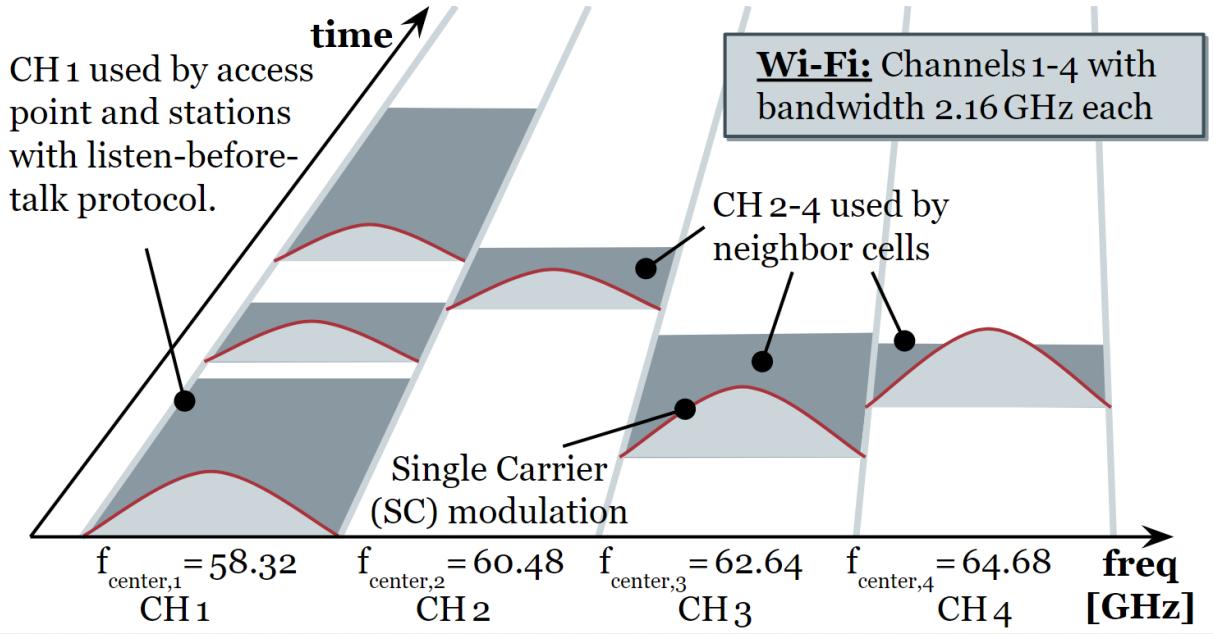

Figure 3: Radio spectrum access and frequency channels of 60 GHz Wi-Fi with SC modulation and coding scheme. Transmitted packets are based on a number of consecutive SC symbols. All evaluations in this study assume operation on channel 2, which ITU-R recommends to be used as default channel, because of its global availability.

3.2. SC Simulation Model

A Bit Error Ratio (BER) model for BPSK and quaternary modulation (QPSK, 16QAM) is applied to determine the code word error ratio and channel capacity in Wi-Fi. The results depend on the selected MCS. A Wi-Fi system typically adapts the MCS dynamically over time, for example to optimize the throughput in the presence of interference (link adaptation). This is included in the simulation model.

Parameter values are taken from Table 2 and Table 3.

3.2.1. Bit Error Ratio (BER)

The BER is given as a function of the Eav/N0 value, which is equivalent to the Signal-to-Noise Ratio.

$$\frac{Eav}{N0} = \frac{S}{N+I}. \qquad \textbf{(Equation 2)}$$

The symbol error ratio P_M for an M-ary QAM for the modulation index $M>2$ is given as

$$P_M = 1 - \left(1 - P_{\sqrt{M}}\right)^2. \qquad \textbf{(Equation 3)}$$

Equation 3 is valid for QPSK and 16QAM modulation, with

$$P_{\sqrt{M}} = 2 \cdot \left(1 - \frac{1}{\sqrt{M}}\right) \cdot Q\left(\sqrt{\frac{3}{M-1} \cdot \frac{Eav}{N0}}\right).$$

For QPSK and 16QAM modulation, the BER is approximated through

$$BER_{QPSK,\ 16QAM} = P_B^{(M)} \approx \frac{P_M}{\log_2(M)},\ M>2.$$

For BPSK modulation, the BER is approximated as

$$BER_{BPSK} = P_B^{(2)} \approx Q\left(\sqrt{2 \cdot \frac{Eav}{N0}}\right).$$

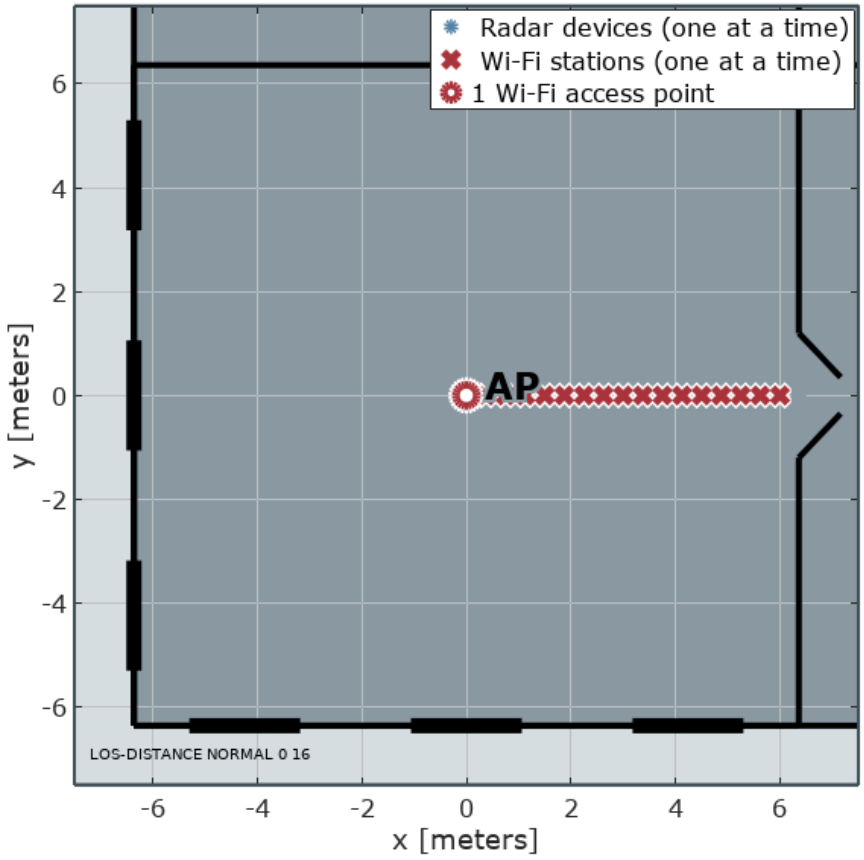

Figure 4: Scenario to demonstrate the performance of the SC MCS. Distances of up to thirty meters are evaluated.

3.2.2. Sensitivity

If the receiving Wi-Fi station is out of the transmitter's coverage range as defined by the cut-off sensitivity levels (Table 3), the BER is set to 100% to set the channel as highly unreliable:

$$BER = \begin{cases} BER & if\ P_{rx} > P_{rx,\,cutoff} \\ 1 & else \end{cases}$$

3.2.3. Code Word (Packet) Error Probability and Channel Capacity

The first-event bit error probability is taken into account. Assuming uncorrelated bit errors,[1] the codeword or Packet Error Ratio, PER, is given by

$$PER = 1 - (1 - BER)^{size\,(codeword)}$$

with code word size measured in *bit*. Table 2 defines the default size. Taking coding gains into account (low-density parity-check estimates as stated in Table 2), the resulting maximum channel capacity now can be defined.

It is affected by a constant overhead resulting from the periodic Golay sequences, and determined as

$$C = Codingoverhead \cdot (1 - PER) \cdot Rate \cdot GolayLoss\,.$$

3.3. Evaluation

The scenario shown in Figure 4 is used to evaluate the performance of the SC modulation. Results are shown over the distance between the transmitting Wi-Fi access point and the receiving Wi-Fi station. For both path loss models, LOS and NLOS, Figure 5 to Figure 9 show the BER, the code word error probabilities, the effect of the cut-off sensitivity level for all 12 MCSs, the resulting channel capacity for all 12 MCSs, and the Wi-Fi throughput obtained by selecting the optimal MCS mode to maximize the achievable Wi-Fi throughput. Radar interference is not included in the model. This is analyzed later in this document (Section 4: model, Section 5: results).

[1] The duration of a block (LDPC encoded data + Golay) is only 290.91 nanoseconds. Therefore, and because the channel model does not consider fading due to mobility or obstacles, it is assumed that the interfering radar signal will always affect all consecutive symbols within one code word (one block) similarly.

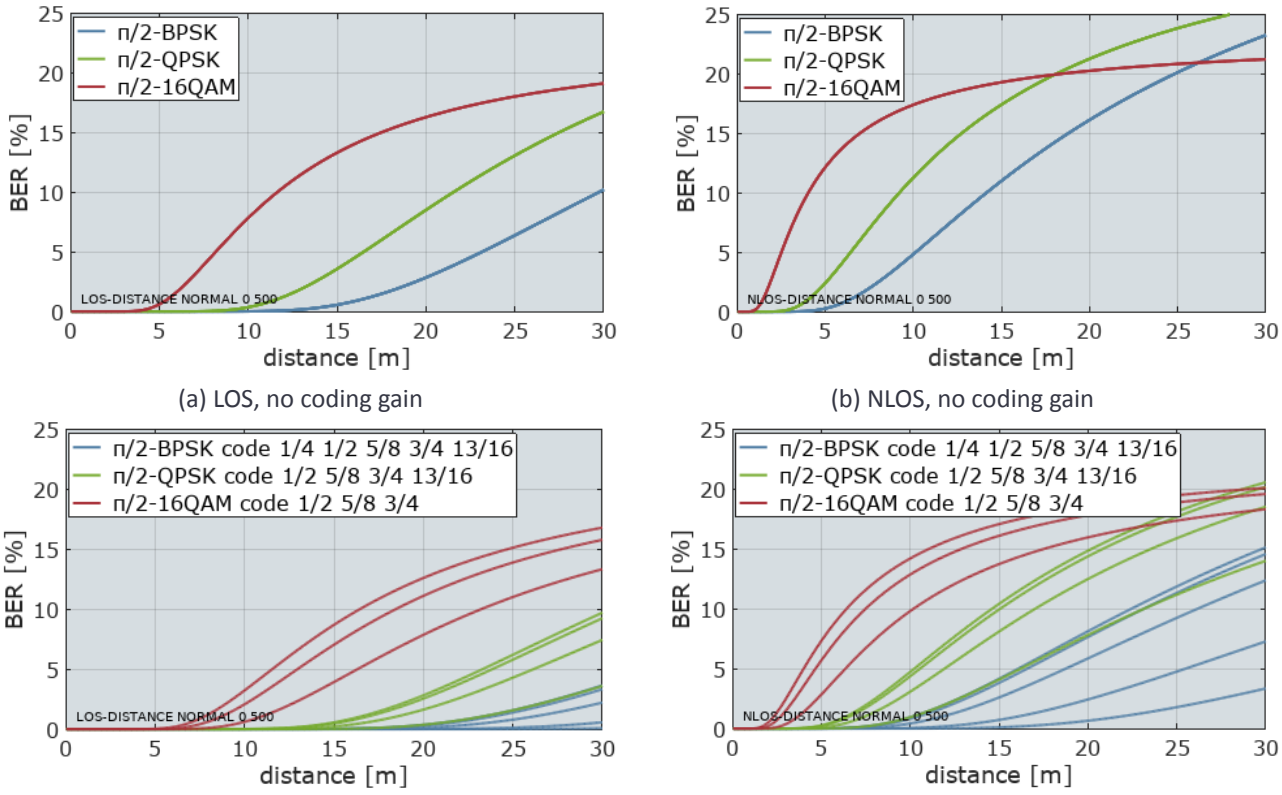

(a) LOS, no coding gain

(b) NLOS, no coding gain

(c) LOS, with coding gain

(d) NLOS, with coding gain

Figure 5: Theoretical Bit Error Ratio (BER) for the three modulations π/2-BPSK, π/2-QPSK, and π/2-16QAM. There is no radar interference. Only thermal noise is considered. Figures (a) and (b) show the theoretical BER for modulation without encoding. MCS 1-12 apply these three modulations by adding encoding. The estimated coding gains are taken into account by adding them to Eav/N0. The two bottom figures (c) and (d) indicate the theoretical BER when coding gains are considered.

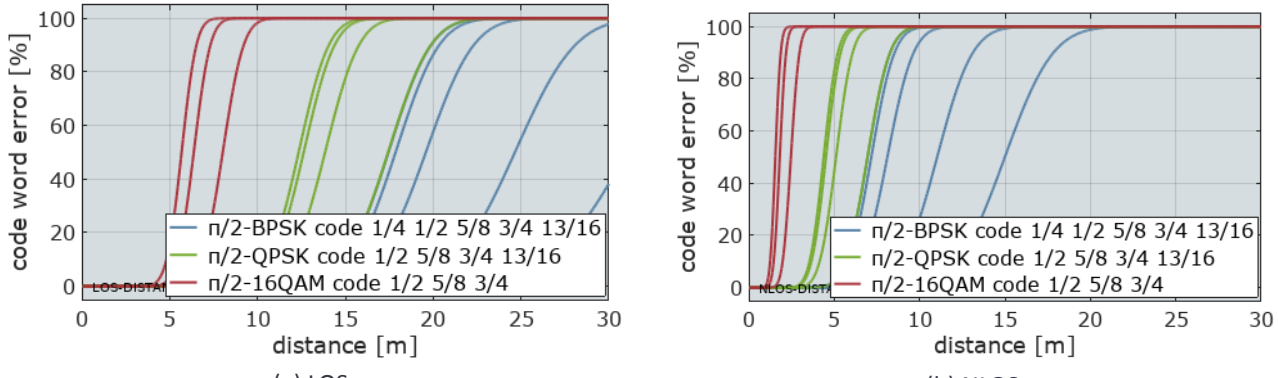

(a) LOS

(b) NLOS

Figure 6: Code word error probabilities for all MCSs, with coding gains.

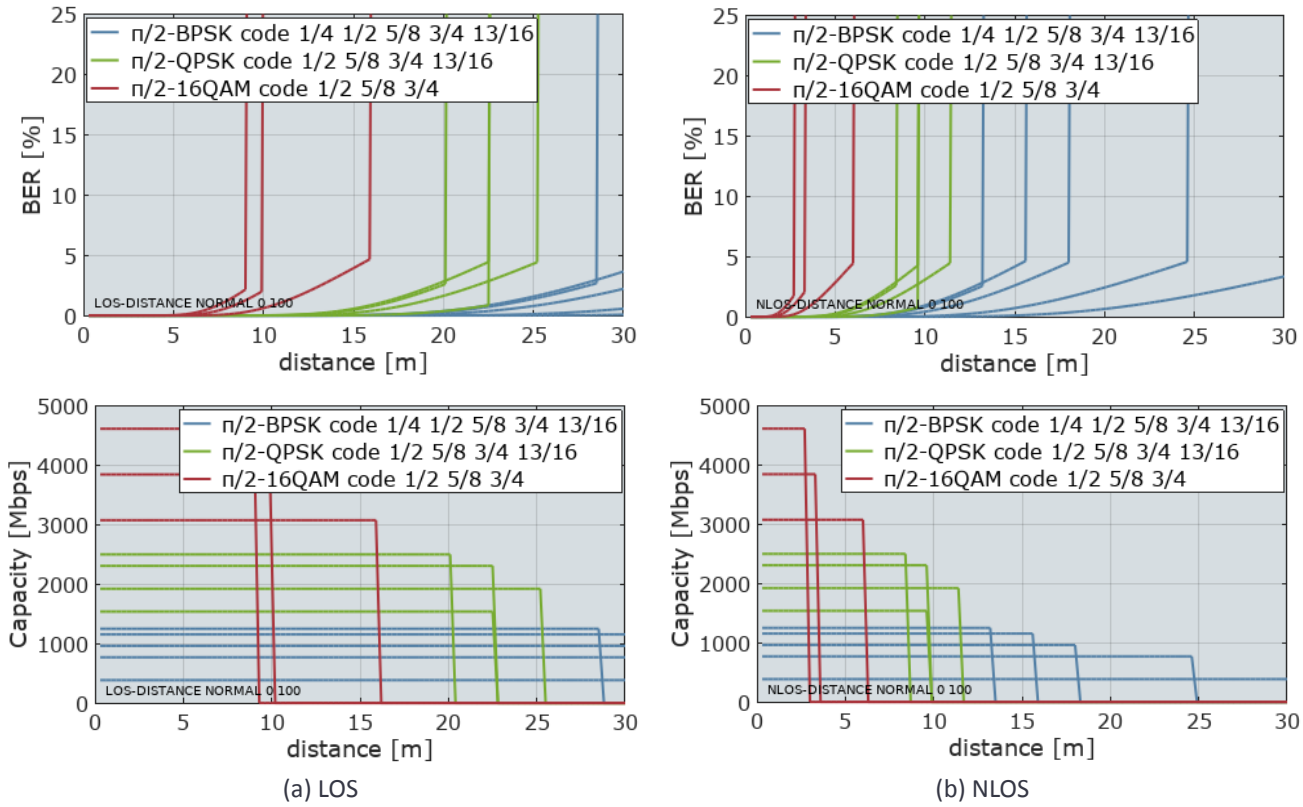

(a) LOS (b) NLOS

Figure 7: BER and capacity results including receiver sensitivity. The receiver sensitivity limits the coverage range of a radio system, but - given the path loss models applied here - this occurs at comparably large ranges.

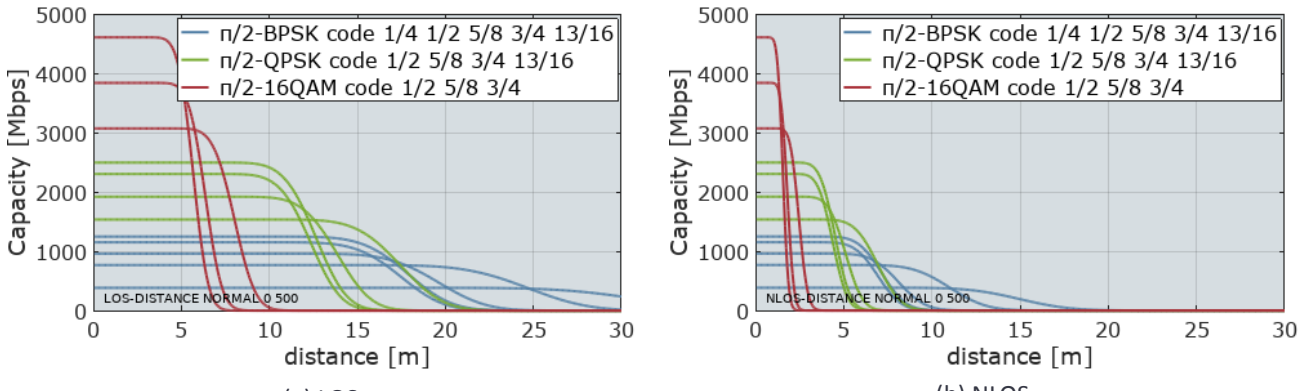

(a) LOS (b) NLOS

Figure 8: The resulting channel capacity for all twelve MCSs. One code word (size 84 byte) is used as packet size. There are no bit errors at short distances, and the capacity is only limited by coding overhead and Golay sequences. Different MCS modes achieve different maximum capacities. More robust MCSs trade the achievable capacity with an increased coverage range (distance). No radar interference, thermal noise only.

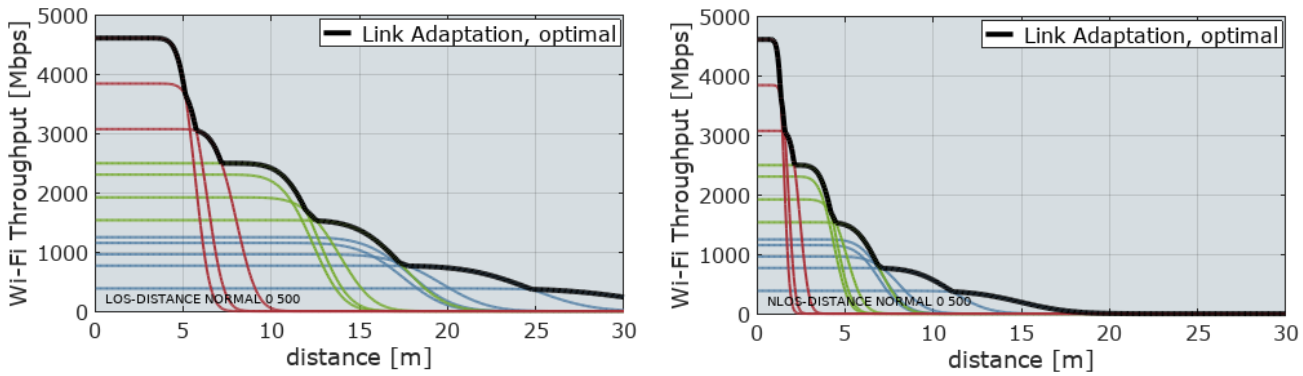

Figure 9: Wi-Fi applies dynamic MCS selection, also referred to as link adaptation. The resulting optimal Wi-Fi link throughput is indicated here. This dynamic MCS selection is the reason for the step-wise shape of some results in later sections. No radar interference, thermal noise only.

4. Interference Model

This section describes how the impact of continuous wave radar interference upon Wi-Fi SC modulation is modelled in this analysis. For the sake of clarity and conservatism, we employ a simplistic approach to modeling this interference, which in fact overemphasizes the effect of such interference on Wi-Fi.

As detailed in Mangold, 2018, the radar sweeps across 7 GHz over a duration of 600 us. As a result, the radar is transmitting within a Wi-Fi channel for approximately only 25% of that sweep time. These effects are illustrated in Figure 10 and Figure 11.

Given the slow speed of the radar sweep relative to the time for a single Wi-Fi symbol (~0.57 ns) or even a block (~290 ns), the radar is in effect a CW interference with constant frequency that is added to the SC modulated Wi-Fi waveform.[2]

The impact of such interference upon SC modulation is studied in detail in Axford (1992).[3] The effect of CW interference is understood by analyzing its effect upon the canonical matched filter-based receiver (at baseband). From first principles, the matched filter output (which at its core is an integration of the received waveform for a symbol period, or 0.57 ns here) is equal to the normal signal constellation plus additive Gaussian noise, plus an additional term equal to the integral of the CW interference over a symbol period. This is captured in Equations 8 and 10 of Axford (1992).

As a result, any CW interference shifts the received signal constellation by an offset. That offset is equal to the integration of the CW interference over the symbol period, and thus depends upon the frequency and phase of the CW interference relative to the Wi-Fi carrier frequency and the symbol timing boundaries, respectively.

[2] The analysis that follows makes it clear that the very small frequency shift that can occur from symbol-to-symbol and across blocks is not consequential, as the key is the radar interference energy that is integrated by the matched filter in each symbol.

[3] The analysis in Axford (1992) covers binary phase-shift keying (BPSK), and thus only considers the in-phase (I) component of the signal. However, the analysis can be extended to complex constellations (π/2-BPSK, π/2-QPSK, π/2-pi/2 16-QAM) in a straightforward manner by considering the matched filter output in both the in-phase (I) and quadrature (Q) components. Axford (1992) focuses on hard decoding of BPSK while Wi-Fi products are expected to employ the more powerful soft-decoding technique; however, degradation due to an increase in the effective noise level affects both hard- and soft-decoding in a similar manner. Axford (1992) also considers traditional SC modulation as opposed to the block-based (blocks of 512 symbols, including a 64-symbol Golay sequence) approach employed in 802.11ad; however, there is nothing inherent to the 802.11ad modulation structure that makes it more vulnerable to narrowband interference than the simpler system in the reference.

Based upon Equation 8 and Figure 6 of Axford (1992), it is evident that the CW interference has no effect (i.e., no shift of the constellation) when the interference is precisely at the edge of the Wi-Fi band, because in that case the CW interference spans its exact period in a Wi-Fi symbol period and thus integrates to zero. As the radar frequency approaches the Wi-Fi carrier frequency, its effect will increase (the integration will be over less than a symbol period of the sinusoidal interference, and thus almost always will be non-zero) and its impact will be maximal when the radar frequency is precisely at the Wi-Fi carrier frequency (again see Figure 6 of Axford, 1992). In this case, the signal constellation is shifted by the full amplitude of the interfering signal. As the radar frequency moves towards the upper end of the Wi-Fi band, its impact will again lessen.

Although the impact of the radar decreases substantially as the instantaneous radar frequency gets farther away from Wi-Fi's carrier frequency (see Figure 6 of Axford, 1992), for the sake of simplicity and in order to maximally model the impact of the radar on Wi-Fi, we assume that the impact of the radar on Wi-Fi (whenever it is in the Wi-Fi channel) is always worst-case, i.e., the frequency of the radar transmission is aligned with the Wi-Fi carrier. Under this counterfactual worst-case assumption, the signal constellation is shifted by a complex constant whose amplitude is equal to the amplitude of the interference (i.e., the square root of the interference power), with a phase determined by the relative phase of the interference (which can be modelled as uniformly distributed over all possible values) to the Wi-Fi carrier.

The final result is that the signal constellation is degraded by the standard thermal noise component (additive Gaussian noise), plus an additional term with random phase and amplitude equal to that of the interference. As is often done, and motivated by the worst-case nature of Gaussian noise,[4] the noise and the new additive term can be modeled by Gaussian noise with power equal to the sum of the thermal noise and the interference power.[5]

While this provides an accurate worst-case modeling of the interference that actually can be expected, in order to be even more conservative and conclusively address concerns regarding the impact of radar interference on Wi-Fi, we further boost the interference power in our analysis by a factor of 5 (i.e., 7 dB) before adding it to the thermal noise. This arbitrary adjustment of +7 dB is factored into throughput results provided later in this report.

[4] *See* Digavi and Cover (2001), and references therein.

[5] While thermal noise is indeed independent across successive data symbols, the additive component due to the radar interference may be correlated across symbols (because successive symbols experience the same sinusoidal interference, but integrated across successive and non-overlapping symbol time periods). The effect of such correlation is alleviated by the interleaving of information bits inherent in the LDPC-based forward-error correction implemented in 802.11ad. The +7 dB adjustment described at the end of this section provides further assurance that any lingering effects are captured by this study.

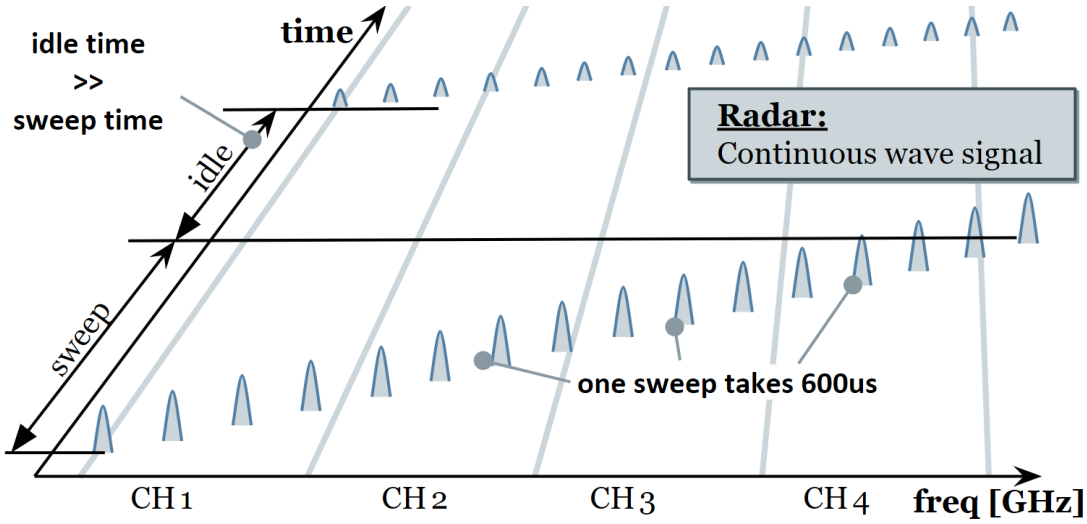

Figure 10: Timing of the radar signal. The idle time is determined by the duty cycle.

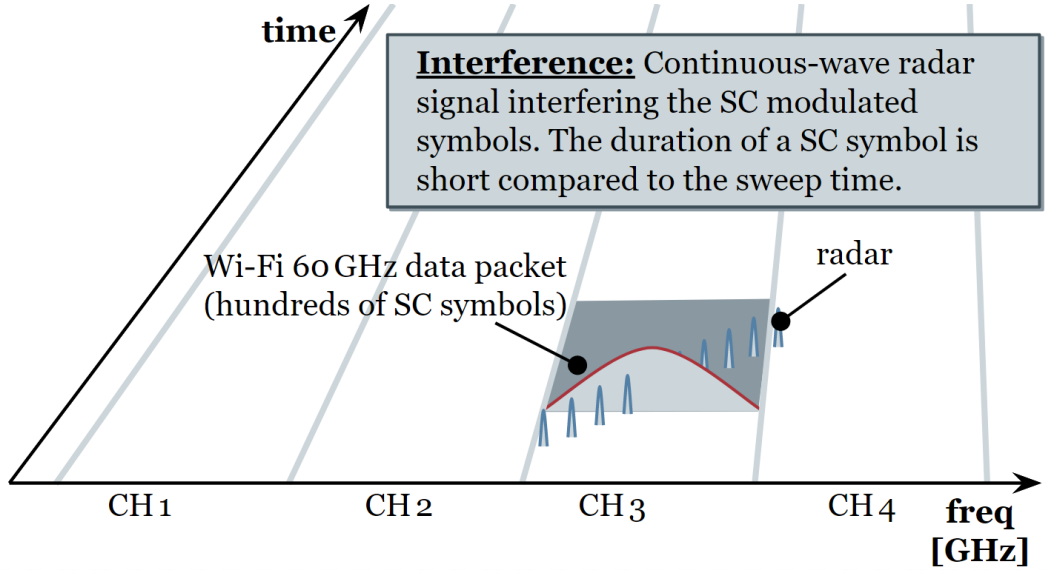

Figure 11: Interference calculation for SC modulation and coding scheme: The CW radar signal is modelled as interferer with random but time-invariant constant frequency offset (off-tuned) and random initial phase shift, during the duration of one SC symbol.

5. Simulation Results

All simulation results relevant to the interference scenarios are presented here. Two different scenarios are used to analyze the coexistence scenarios, see Figure 12.

(a) TYPICAL: Random locations for radar devices and Wi-Fi stations, covering all possible configurations. LOS and NLOS path loss models are used.

(b) SHORT_RANGE: Line of Wi-Fi stations with distances to the access point around half of the room width, with a radar interferer arbitrarily centered around the station, at short distance. Again, LOS and NLOS path loss models are used.

The simulation results presented in the remainder of this section (Figure 13 and Figure 14 for TYPICAL and Figure 15 and Figure 16 for SHORT_RANGE) focus on the same performance indicators as in the first study (received power, signal-to-noise ratio, channel capacity).

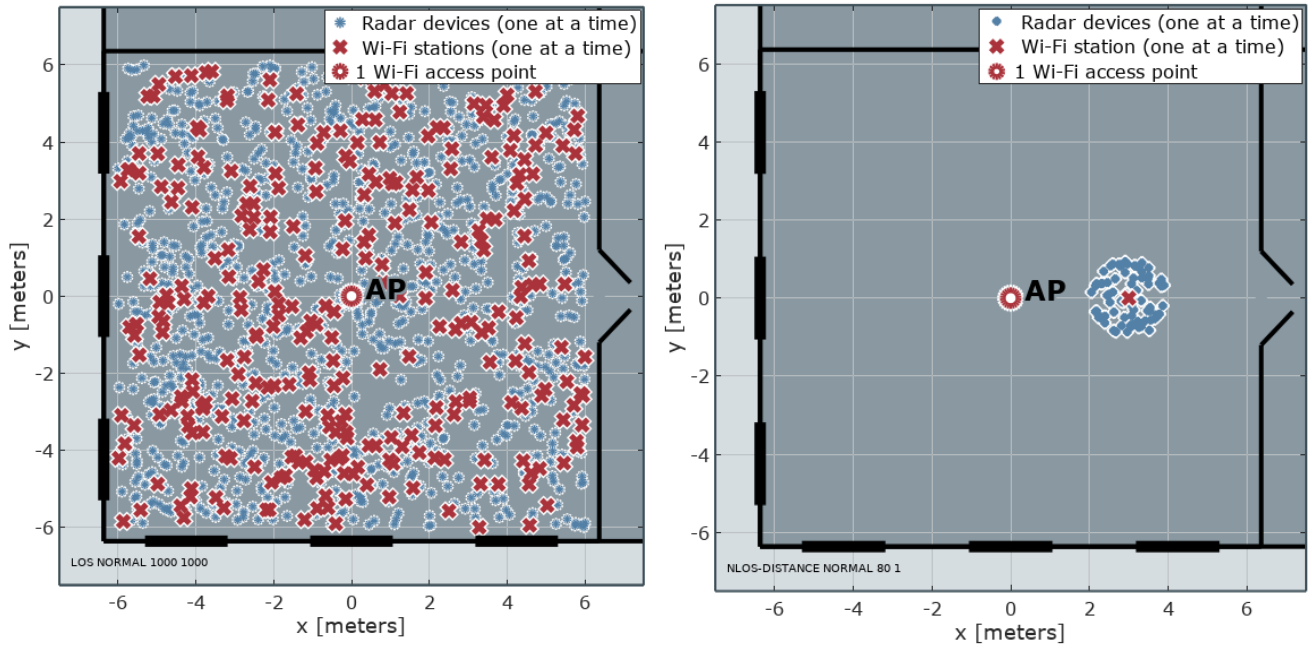

(a) "TYPICAL" with full room coverage. Channel model: LOS or NLOS.

(b) "SHORT_RANGE" Channel model: LOS or NLOS.

Figure 12: Simulation scenarios. There are always only three devices in each simulation experiment: One Wi-Fi AP, one Wi-Fi station, and one radar device. The Wi-Fi antennas always point to each other. The radar antenna always points to a randomly selected direction and therefore the radar's main beam may or may not hit the main beam of the Wi-Fi receiver.

5.1. Scenario TYPICAL

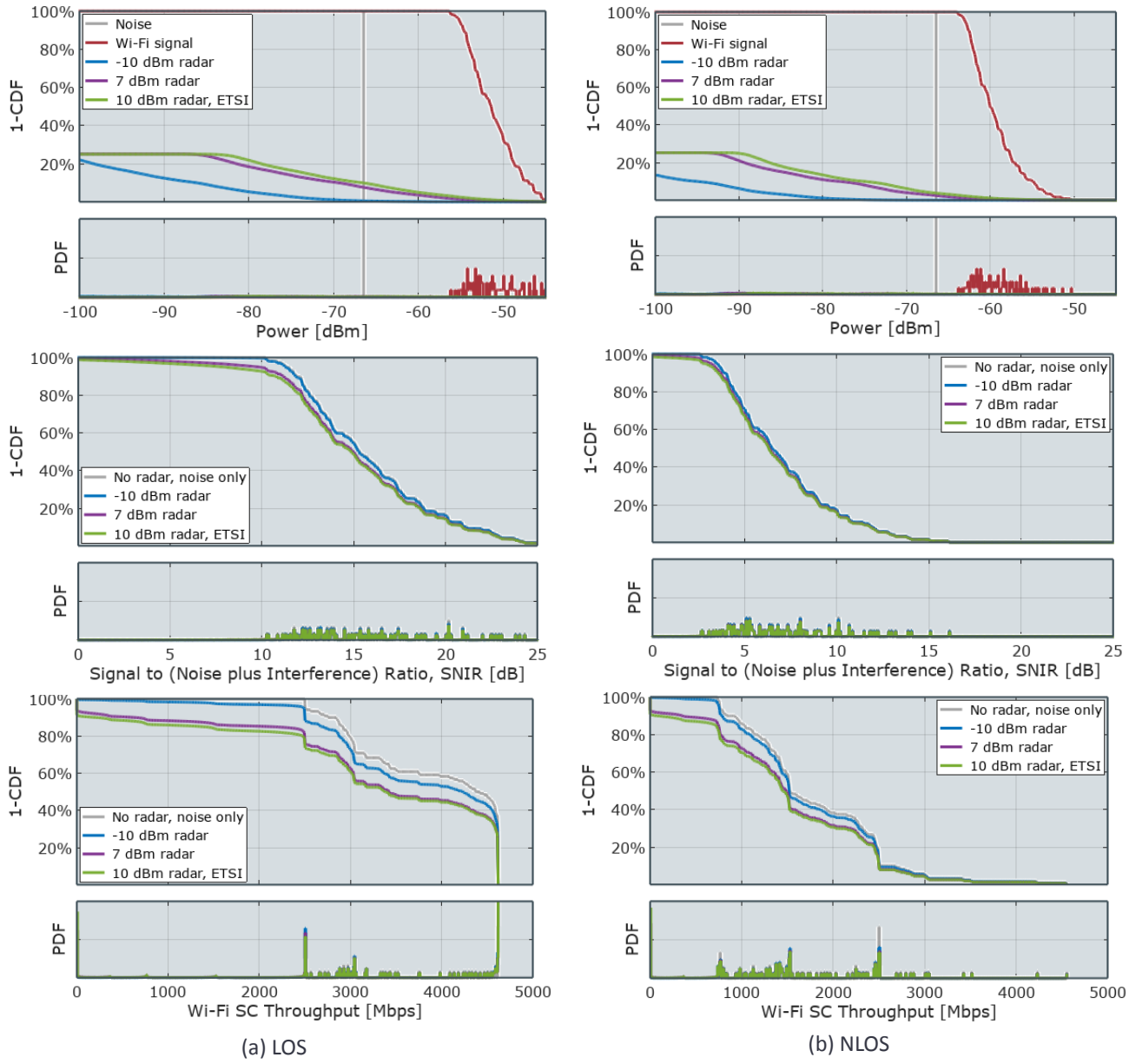

Figure 13: Simulation results for the scenario "TYPICAL" with the radar device always active.

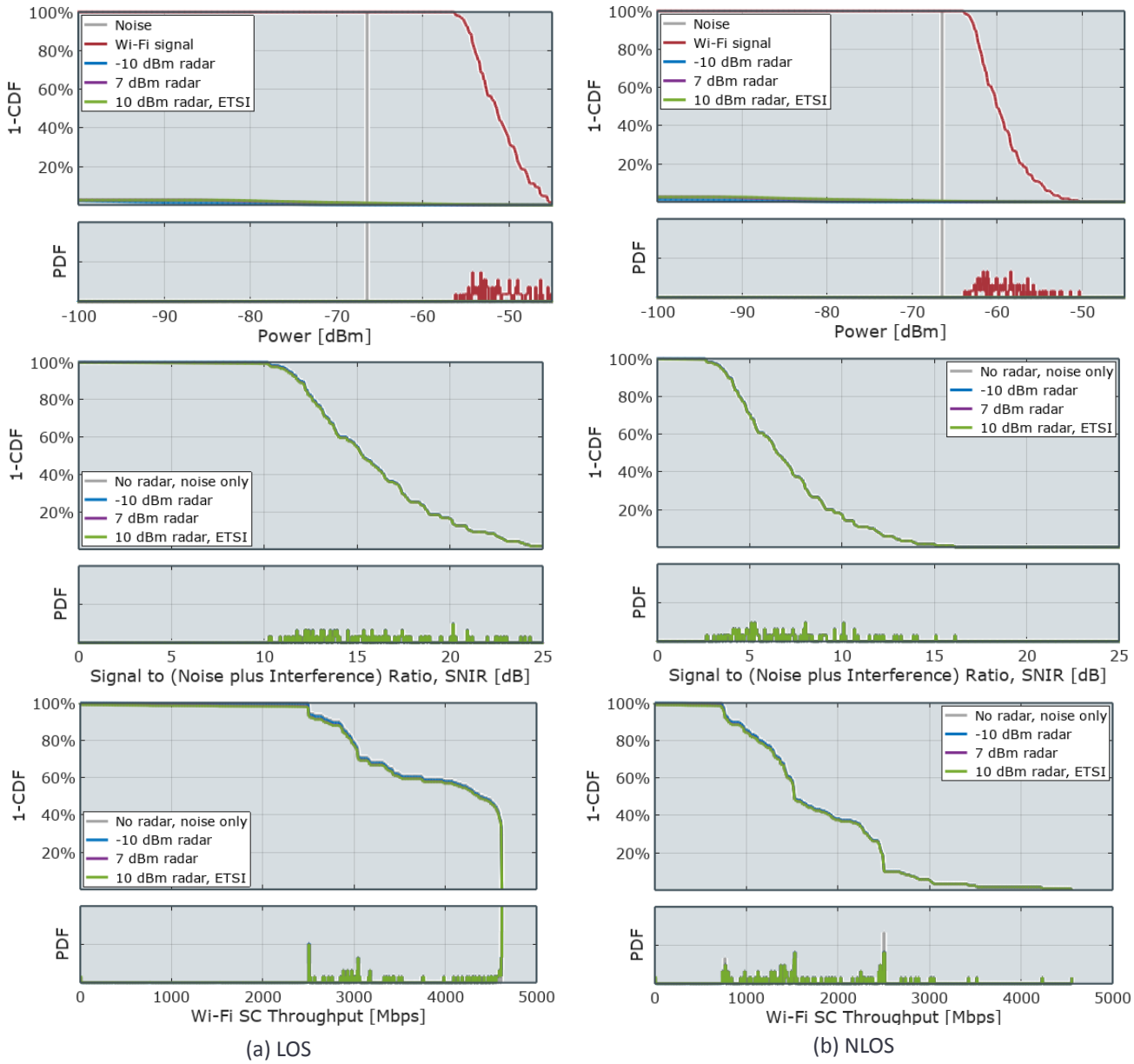

Figure 14: Simulation results for the scenario "TYPICAL" with a 10% transmit duty cycle, a conservative analysis of the expected maximum.

Figure 13 and Figure 14 show the simulation results for the scenario TYPICAL, for the LOS path loss model on the left, and the NLOS path loss model on the right. The results in Figure 14 are produced with a duty cycle of 10%. Three performance indicators are evaluated. The power of the received signals (desired Wi-Fi and interfering radar signals) at the location of the Wi-Fi station are shown in

the two figures at the top. The resulting signal to noise ratio can be found in the middle graphs, and the channel capacity or Wi-Fi throughput is shown in the bottom figures.

Multiple effects can be observed. In around 75% of the simulations, as clearly visible in the top figures, the radar operates out of band without creating any substantial interference. Together with a potential misalignment of the radar and Wi-Fi antennas (i.e., it is possible that the radar main beam would not hit the main beam of the Wi-Fi receiver), the overall resulting effect is negligible. The Wi-Fi receiver performance is not significantly compromised, regardless of the power level at which the radar is operating (-10 dBm, 7 dBm, or 10 dBm).

There are however small observable effects on Wi-Fi performance as a result of interference from the radar. With increased radar signal power, Wi-Fi is affected by up to 10% throughput reduction in the worst case.

Figure 14 shows that duty cycling mitigates the effect of the radar interference.

Overall, the radar's impact is less significant in NLOS scenarios compared to LOS. This is partially due to the fact that independent shadow fading is not taken into account in the NLOS channel models. The NLOS channel simply attenuates all signals strongly, without independent variations (radar signal and Wi-Fi signal are equally affected). Independent fading could occur in real life, but is assumed less likely here, given the short distances between the devices (in the order of meters) and the potential size of possible obstacles.

The stepwise shape of the capacity Wi-Fi throughput graphs in the two bottom figures results from the applied link adaptation.

5.2. Scenario SHORT_RANGE

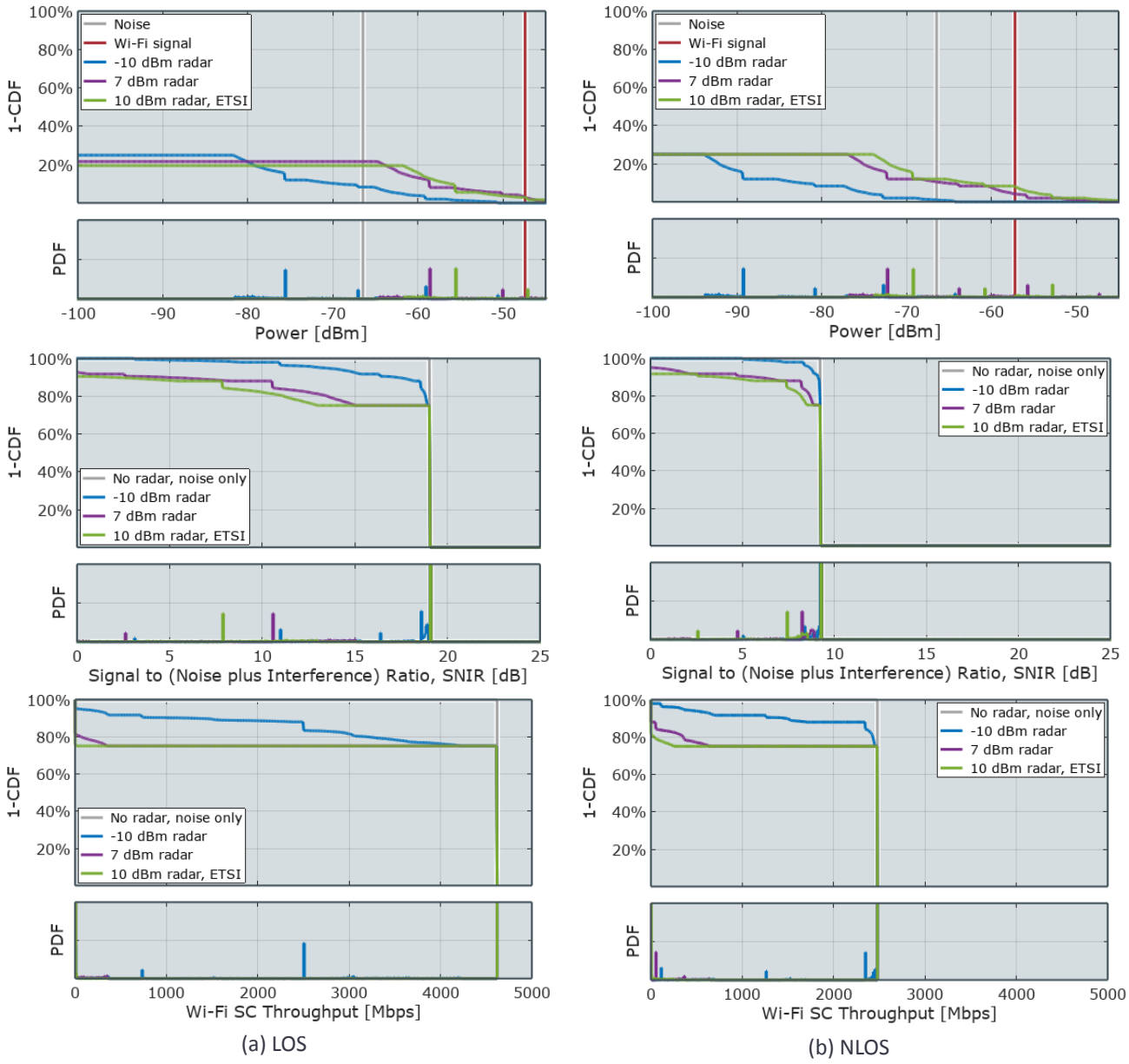

Figure 15: Simulation results for the scenario "SHORT_RANGE" with the radar device always active.

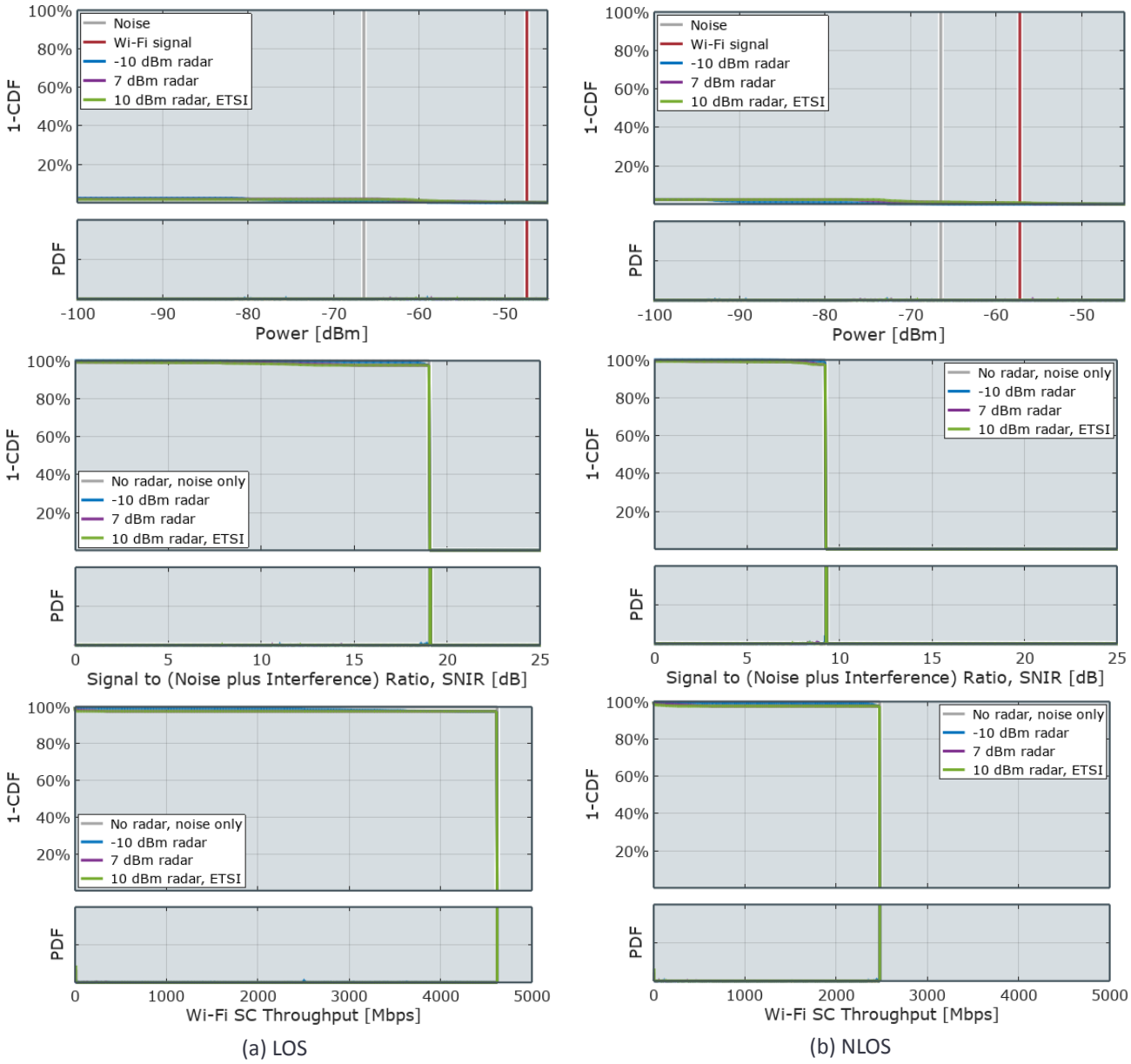

Figure 16: Simulation results for the scenario "SHORT_RANGE"with a 10% transmit duty cycle, a conservative analysis of the expected maximum.

The results of the scenario SHORT_RANGE are shown in Figure 15 for the radar device being always active, and Figure 16 for a 10% transmit duty cycle.

The effect of the out of band operation of the radar is more visible in the short range scenario. In around 75% of the experiments, the radar operates out of band without creating interference at all.

The shown Wi-Fi throughput in the bottom figures of Figure 15, however, indicates that radar devices located very closely to a receiving Wi-Fi station with the radar device always active will result in a level of interference that affects the channel capacity (if the affected Wi-Fi station is receiving from an AP further away), at around 5% to 20% of all simulations. There is, however, no significant effect on the channel capacity if the radar device operates at 10% transmit duty cycle (Figure 16).

The presented scenario is the worst case scenario, limiting the channel's availability in 10% to 20% of all simulations, if the radar device is always active. Conversely, in up to 80% to 90% of the simulations, Wi-Fi communication will not be affected at all even if the radar device is always active. And, as noted, there is no significant effect on the channel capacity when the radar device is assumed to operate at 10% transmit duty cycle.

Because of the relatively short distances between devices simulated in this scenario, similar results are obtained when changing the path loss model from LOS to NLOS (the figures for LOS, left, and NLOS, right, show the same effect).

6. Model Validation

The study in Jiang (2018) contains laboratory measurement results produced with commercially available off-the-shelf 60 GHz Wi-Fi devices. Some of the findings of the study can be used to validate the simulation model of this supplementary study.

Figure 17 shows the setup and the resulting throughput results for comparable scenarios. The Wi-Fi station is located at a distance of 15.24 meters (50 ft) away from the transmitting access point. Among other traffic configurations, downlink-only best effort (with and without interference from a co-located radar device) is used here to test if the outcome of the simulation matches the measurement.

Results are shown in Figure 17 and Table 5. For **SCENARIO 0** (no radar), the simulation model predicts slightly higher throughput outcomes for the LOS channel model (around 1300 Mbps instead of 940 Mbps). This can be explained with protocol overhead, for example the Wi-Fi listen-before-talk medium access, small packet sizes leading to control overhead, or retransmissions and sliding windows on the network layer (O'Hara and Petrick, 2005). Note that the throughput measurements were taken on the IP network layer instead of the physical layer.

Jiang et.al. (2018) defines three more scenarios that include a co-located radar for different antenna alignments and distances:

- **SCENARIO 1:** Radar directly pointing from short distance into the main beam of the Wi-Fi station's antenna
- **SCENARIO 2:** Varying short distances between radar and Wi-Fi station, and varying radar antenna directions
- **SCENARIO 3:** Radar flat on the table, at varying distances, with the radar device not necessarily pointing toward the main beam of the Wi-Fi antenna

The simulation model takes radar duty cycles and out-of-band operation into account. Therefore, the moderate effect of the radar on the Wi-Fi throughput in **SCENARIO 2** and **SCENARIO 3** are reasonably approximated. **SCENARIO 1**, however, shows the limitation of the simulation model for extreme outlier cases with heavily aligned antennas. This is not unexpected, as the antenna near fields are not modelled, and possible dynamic effects of link adaptation (changes of MCS) or protocol behaviors such as retransmissions are not taken into consideration in the simulation model.

More details about the measurement scenarios and radar system setup (e.g., duty cycle, emission power) are provided in Jiang et.al. (2018).

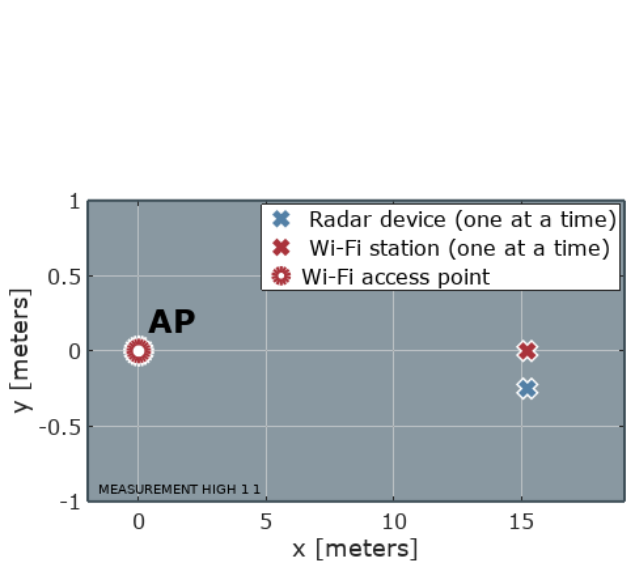

(a) Scenario

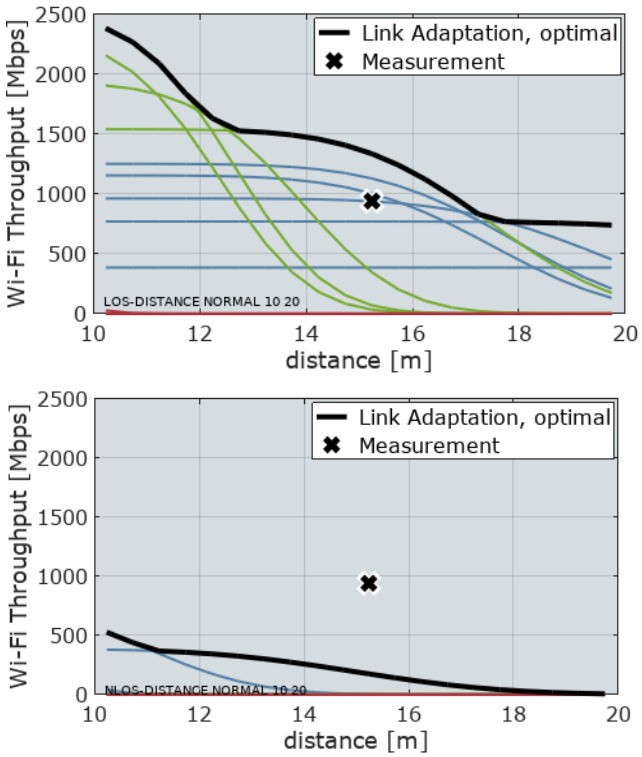

(b) Throughput results for LOS (top) and NLOS channel model (bottom)

Figure 17: Downlink measurement scenario (a, left), and throughput results for LOS and NLOS (right).

Scenario	Measured IP Layer Downlink Throughput (Jiang et.al., 2018)	Simulated Physical Layer Downlink Throughput
0	941 Mbps	1335.4 Mbps ✔
1	461 … 666 Mbps	**1322.1 Mbps ✖**
2	803 … 939 Mbps	1322.1 Mbps ✔
3	901 … 937 Mbps	1322.1 Mbps ✔

Table 5: Measurement and simulation results for downlink traffic in the scenarios described in Jiang et.al. (2018).

7. Summary and Final Remarks

This study analyzes interference effects of a radar system on 60 GHz Wi-Fi with the help of radio channel and system models. The approach is based on standard link budget models that are typically used for assessing the quality of a wireless link, or for evaluating spectral coexistence between radio systems. The Wi-Fi model presented in this study contains the IEEE 802.11ad single carrier modulation and coding schemes.

Coexistence simulation results are shown for a line-of-sight path loss channel model and a non-line-of-sight model. Both path loss models are derived from models used in literature.

This work is intended to advance discussions concerning spectral coexistence between radars and Wi-Fi at 60 GHz, while remaining simple enough to allow readers to evaluate the full model. Despite the simplicity of the simulation model, the validation in Section 6 demonstrates that the simulated throughput results are consistent with the reported outcome of laboratory tests with commercially available IEEE 802.11ad equipment.

The main findings of this supplemental study are found in Section 5. Overall, the results predict a low level of interference and confirm the results of the first study. For the given indoor scenario and with both path loss channel models, the Wi-Fi throughput is only marginally affected by interference from the radar (around 10% throughput reduction at most, if any at all). The radar duty cycling further helps to efficiently protect the operation of 60 GHz Wi-Fi. In outlier short range scenarios with co-located devices in close proximity to each other, a radar interferer can create additional interference, but only during in-band operation (around 25% of the experiments) and with the radar device always active. This effect can be greatly mitigated by radar duty cycling.

References

AXFORD (1992) **Effects of CW- and BPSK-Signal Interference on a Standard BPSK Digital Communications System**. Technical Report 1510, Naval Command, Control, and Ocean Surveillance Center RDT&E Division, Aug. 1992. www.dtic.mil/dtic/tr/fulltext/u2/a255617.pdf [accessed in 2018-04].

DIGAVI AND COVER (2001) **The worst additive noise under a covariance constraint**. IEEE Transactions on Information Theory, Vol. 47, Issue 7, Nov. 2001. ieeexplore.ieee.org/document/959289 [accessed in 2018-06]

IEEE 802.11AD (2014) **Enhancements for very high throughput in the 60 GHz band (adoption of IEEE Std 802.11ad-2012)**. ISO/IEC/IEEE Standard 8802-11:2012/Amd 3:2014, 2014. www.iso.org/iso/home/store/catalogue_tc/64876 [accessed in 2018-04].

IEEE 802.11 (2016) **IEEE Standard for Information technology--Telecommunications and information exchange between systems Local and metropolitan area networks--Specific requirements - Part 11: Wireless LAN Medium Access Control (MAC) and Physical Layer (PHY) Specifications**. IEEE Std 802.11-2016 (Revision of IEEE Std 802.11-2012), Dec. 14, 2016. doi:10.1109/IEEESTD.2016.7786995 [accessed in 2018-04].

JIANG AND NIJJAR AND JINDAL AND HUSTED AND WEBER (2018) **Measurement Study on Soli/11ad Coexistence.** Submission to FCC. Google LLC, May 2018.

MALTSEV AND PERAHIA AND MASLENNIKOV AND SEVASTYANOV AND KHORYAEV (2008) **60 GHz WLAN Experimental Investigations**. IEEE 802.11 Working Document 11-08/1044r0, Sep. 2008. mentor.ieee.org/802.11/dcn/08/11-08-1044-00-0vht-60-ghz-wlan-experimental-investigations.ppt [accessed in 2018-04].

MALTSEV AND ERCEG AND PERAHIA AND HANSEN AND MASLENNIKOV AND LOMAYEV AND SEVASTYANOV AND KHORYAEV AND MOROZOV AND JACOB AND PRIEBE AND KÜRNER AND KATO AND SAWADA AND SATO AND HARADA (2010) **Channel Models for 60 GHz WLAN Systems**. IEEE 802.11 Working Document 11-09/334r8, May 2010. mentor.ieee.org/802.11/dcn/09/11-09-0334-08-00ad-channel-models-for-60-ghz-wlan-systems.doc [accessed in 2018-04].

MANGOLD (2018) **Assessing the Interference of Miniature Radar on Millimeter Wave 60 GHz Wi-Fi**. Simulation study. Lovefield Wireless GmbH, Feb-21, 2018. ecfsapi.fcc.gov/file/ 103071586588 94/ 2018-03-07 Soli Request for Waiver - Simulation Study.pdf [accessed in 2018-04].

NITSCHE AND CORDEIRO AND FLORES AND KNIGHTLY AND PERAHIA AND WIDMER (2014) **IEEE 802.11ad: Directional 60 GHz Communication for Multi-Gigabit-per-Second Wi-Fi**. IEEE Communications Magazine, vol. 52, no. 12, pp. 132-141, Dec. 2014. doi:10.1109/MCOM.2014.6979964 [accessed in 2018-04].

O'HARA AND PETRICK (2005) **IEEE 802.11 Handbook: A Designer's Companion**. New York USA: John Wiley & Sons, Inc.. 2nd Edition. ISBN: 978-0-738-14449-8.

PERAHIA AND GONG (2011) **Gigabit wireless LANs: an overview of IEEE 802.11ac and 802.11ad**. SIGMOBILE Mob. Comput. Commun. Rev. 15, 3 (Nov. 2011), 23-33. DOI=dx.doi.org/ 10.1145/2073290.2073294 [accessed in 2018-04].

RAPPAPORT (2008) **Wireless communications: principles and practice**. Upper Saddle River, New Jersey: Prentice Hall. 2nd Edition. ISBN: 0-13-042232-0. ISBN-13: 9780130422323.

SANDERS (2012) **The Rabbit Ears Pulse-Envelope Phenomenon in Off-Fundamental Detection of Pulsed Signals**. NTIA Technical Report TR-12-487, July 2012. www.its.bldrdoc.gov/publications/ 2678.aspx [accessed in 2018-04]

SANDERS, F. AND CARROLL AND SANDERS, G. AND SOLE (2013) **Effects of Radar Interference on LTE Base Station Receiver Performance**. NTIA Technical Report TR-14-499, Dec. 2013. www.ntia. doc.gov/report/2013/effects-radar-interference-lte-base-station-receiver-performance [accessed in 2018-04].

Appendix A: Erratum to Mangold (2018)

Page 14 states:

> "*The FMCW radar signal sweeps through a broader spectrum than one Wi-Fi channel and creates interference only at a fraction of time. However, the sweep time is short. To sweep through one Wi-Fi channel takes less time than the duration of one Wi-Fi OFDM symbol duration (~242 us, see Table 1). Hence, a Wi-Fi data packet transmission is usually affected by multiple repeated sweeps. For this reason, the out-of-channel time is ignored and a continuous interference (worst case assumption) is assumed.*" [Mangold, 2018]

This statement is not correct. One Wi-Fi OFDM symbol duration is around 242 nanoseconds, and not 242 microseconds as stated in the quoted text. It is therefore not possible that multiple repeated sweeps from the same radar device will affect one OFDM symbol. The assumption that there will always be interference on the frequency channel is therefore too pessimistic, even if the radar device were always to be active. Instead, in only 1 out of 4 experiments (around 25% probability), the Wi-Fi channel under investigation will be affected at all. This is taken into account in the supplemental study.

Appendix B: Implementation Details

```
function samples_W = estimate_interference(x_radars, y_radars, x_WiFi, y_WiFi, P_Tx_radar_W, Gt, Gr,
isNlos, ANTENNACONFIG)

 I = [];
 radar_positions = [];
 samples_W = [];

 for wificnt = 1:size(x_WiFi,2)
  samples01_W = []; % this construct is needed to speed up the simulation

  for radarcnt = 1:size(x_radars,2)
  switch ANTENNACONFIG
     case "HIGH"
        one_P_Tx_radar_W = P_Tx_radar_W;
        one_Gr = Gr;
     case "NORMAL"
        if rand < .66666667 % Given the antenna pattern of the radar device (-60..+60 degree), in 66%,
                            % P_Tx_radar is reduced. Impact will be minimal.
           one_P_Tx_radar_W = P_Tx_radar_W .* ( 10.^((Gt_reverse_Radar_dBi-Gt_Radar_dBi)./10));
        else
           one_P_Tx_radar_W = P_Tx_radar_W; % this is the direct hit case, maximum impact on Wi-Fi.
        end
        if rand < .75 % in 75%, Gr_WiFi is reduced to 0dBm:
           one_Gr = 0; % this is the Wi-Fi reverse case with minimal impact.
        else
           one_Gr = Gr; % this is the direct hit case on the Wi-Fi receiver, with maximum impact on Wi-Fi
        end

        if rand > FreqCollisionProb % 7000MHz/1760MHz ... Gr_WiFi is reduced to -100dBm
           one_Gr = -100; % this is the OUT OF BAND OPERATION.
         end
     case "LOW"
        one_P_Tx_radar_W = P_Tx_radar_W .* ( 10.^((Gt_reverse_Radar_dBi-Gt_Radar_dBi)./10));
        one_Gr = 0;
     otherwise
        error ("unknown config for ANTENNACONFIG");
     endswitch

     [rx_W] = rxpower(one_P_Tx_radar_W, x_radars(radarcnt), y_radars(radarcnt), x_WiFi(wificnt), ...
                 y_WiFi(wificnt),Gt,one_Gr, isNlos);
     samples01_W = [samples01_W rx_W'];

  end

  samples_W = [samples_W samples01_W];

endfunction
```

Code 1: Interference estimation.

```
function [C_bps100_max C_bps2000_max C_bps100 C_bps2000 Eav2N0 BER PER100 PER2000] =
    capacity_SC(P_Rx_W,I_W,N_W)
        for mcs_cnt = 1:size(ScSensitivity_W,2)
        outofSensitivityRange(1,:,mcs_cnt) = P_Rx_W < ScSensitivity_W(mcs_cnt);
        endfor
        %% ---- Continues Wave interference instead of Gaussian noise
        I_W = I_W .* 50;
        if ~isempty (I_W)
                        Eav2N0 = P_Rx_W ./ (I_W + N_W);
        else            Eav2N0 = P_Rx_W ./ N_W;
        endif
        ScCodingGain    (1,1,:) = 10.^ (ScCodingGain_dB(ScModulationIndex2 ...
                                +1:size(ScModulationIndexM,2))/10);
        ScCodingGainBPSK(1,1,:) = 10.^ (ScCodingGain_dB(1:ScModulationIndex2)/10);
        %% ---- M>2 (QPSK, 16QAM)
        ScModulationIndexM_QAM = ScModulationIndexM(ScModulationIndex2+1: ...
             size(ScModulationIndexM,2)); % take out all BPSK, M=2
        ScModIndex (1,1,:) = ScModulationIndexM_QAM;
        P_sqrtM = 2 .* (1 - 1 ./ sqrt(ScModIndex)) .* ...
            Q(sqrt(3 ./ (ScModIndex-1) .* Eav2N0 .* ScCodingGain)); %Symbol Error Rate P_sqrt(M)
        P_M = 1 - (1-P_sqrtM).^2; %Symbol Error Prob (QAM): P_M = 1-(1-P_sqrt(M))^2
        BER_QAM = P_M ./ log2(ScModIndex); % Bit Error Ratio BER(M)=1/log2(M) * P_M

        %% ---- M=2 (BPSK)
        BER_BPSK = Q(sqrt(2 .* Eav2N0 .* ScCodingGainBPSK));
        % Bit Error Ratio (BER)(BPSK): BER(2) - directly from Eb/N0

        %% ---- putting all modulations together into BER:
        BER (:,:,1:ScModulationIndex2) = BER_BPSK;
        BER (:,:,ScModulationIndex2+1:ScModulationIndex2+size(ScModulationIndexM_QAM,2)) = BER_QAM;
        %% ---- when the device is out of coverage range, we set BER to 1
        BER = max(BER,outofSensitivityRange);
        %% --- Packet Error Ratio PER n
        CodeWordSize_bit = [672 2000]; % code word length, 100 byte = 800 bit. 672 is default
        PER100  = 1 - (1-[BER]).^CodeWordSize_bit(1);
        PER2000 = 1 - (1-[BER]).^CodeWordSize_bit(2);
        for cnt_a = 1:size(PER100,1)
                for cnt_b = 1:size(PER100,2)
                        codes(cnt_a,cnt_b,1:size(ScCodingOverhead,2)) = ScCodingOverhead;
                        rate(cnt_a,cnt_b,1:size(ScMaxDatarate_bps,2)) = ScMaxDatarate_bps;
        end     end
        %% --- Resulting Link Throughput in b/s
        C_bps100  = (codes) .* (1-PER100)  .* rate;
        C_bps2000 = (codes) .* (1-PER2000) .* rate;
        C_bps100  = C_bps100 * ScGolayLoss;
        C_bps2000 = C_bps2000 * ScGolayLoss;
        C_bps100_max = max(C_bps100,[],3);      %% link adaptation
        C_bps2000_max = max(C_bps2000,[],3);
endfunction
```

Code 2: Single Carrier MCS Model

```
function [Rx_W] = rxpower(Tx_W,x_Tx,y_Tx,x_Rx,y_Rx,Gt,Gr, isNlos)
        distance_m = sqrt((x_Tx-x_Rx) .^2 + (y_Tx-y_Rx).^2);
        distance_m = max(distance_m,.5);  # assume distance>d0

        if isNlos AA = 44.7; nn = 1.5;
        else AA = 32.5; nn = 2;  end

        ploss_dB = AA + 20 .* log10(60.48) + 10 .* nn .* log10(distance_m); % from 802.11ad
        Tx_dBW = 10 * log10 (Tx_W);
        Rx_dBW = Tx_dBW - ploss_dB + Gt + Gr;
        Rx_W = 10 .^ (Rx_dBW ./ 10);
endfunction
```

Code 3: Path loss model.